



Title	Docking Strategy To Construct Thermostable, Single-Crystalline, Hydrogen-Bonded Organic Framework with High Surface Area
Author(s)	Hisaki, Ichiro; Suzuki, Yuto; Gomez, Eduardo et al.
Citation	Angewandte Chemie International Edition. 2018, 57(39), p. 12650-12655
Version Type	AM
URL	https://hdl.handle.net/11094/92591
rights	© 2018 Wiley-VCH Verlag GmbH & Co. KGaA.
Note	

The University of Osaka Institutional Knowledge Archive : OUKA

<https://ir.library.osaka-u.ac.jp/>

The University of Osaka

Docking Strategy to Construct Thermostable, Single-crystalline, Hydrogen-bonded Organic Framework with Large Surface Area

Ichiro Hisaki,^{*[a]} Yuto Suzuki,^[a] Eduardo Gomez,^[b] Boiko Cohen,^[b] Norimitsu Tohnai,^[a] and Abderrazzak Douhal^{*[b]}

Abstract: Enhancement of thermal and chemical durability and an increase of surface area are two main directions for the construction and improvement of the performance of porous hydrogen-bonded organic frameworks (HOFs). Herein, we propose that a hexaazatriphenylene (HAT) derivative, which possesses six carboxyaryl groups, is a suitable building block for the systematic construction of thermally and chemically durable HOFs with large surface area due to shape-fitted docking between the HAT cores and interpenetrated three-dimensional network. We demonstrate that a HAT derivative with carboxybiphenyl groups (CBPHAT) forms a stable single-crystalline porous HOF (CBPHAT-1a) that possesses protic solvent durability, even for concentrated HCl, heat resistance up to 305 °C, and a high Brunauer-Emmett-Teller surface area [SA_(BET)] of 1288 m² g⁻¹. A single crystal of CBPHAT-1a has anisotropic fluorescence, which suggests that it would be applicable to polarized emitters based on robust functional porous materials.

Porous organic frameworks have attracted much attention in the fields of materials chemistry and crystal engineering.^[1] Both the structural and electronic versatility of organic molecules enable the functionality of these frameworks to be tuned for applicability as selective gas storage/separation materials, catalysts, chemical sensors, molecular rotors and optoelectronic materials.^[2] Covalent organic frameworks (COFs) are widely investigated for such applications due to their shape-persistent rigid frameworks connected through covalent bonds and high designability from structural and electronic aspects.^[3,4] However, the crystallinity of many COF systems is insufficient,^[5,6] which prevents precise discussion of the structure-property relationships.^[7]

Hydrogen-bonded organic frameworks (HOFs), on the other hand, are available as highly crystalline materials (single crystals in many cases) via a simple recrystallization process because reversible H-bonding allows self-repair of irregular molecular connections, which enables precise structural elucidation by single-crystal X-ray diffraction (SXRD) analysis.^[8] However, such reversibility and the weakness of H-bonds frequently cause the collapse of the frameworks after desolvation, so there is a lack of a universalistic design strategy for HOFs. To resolve these problems, well-designed supramolecular synthons^[9] have been applied,^[10] such as benzimidazolone,^[10h] pyrazole,^[10i,j] the 2,4-

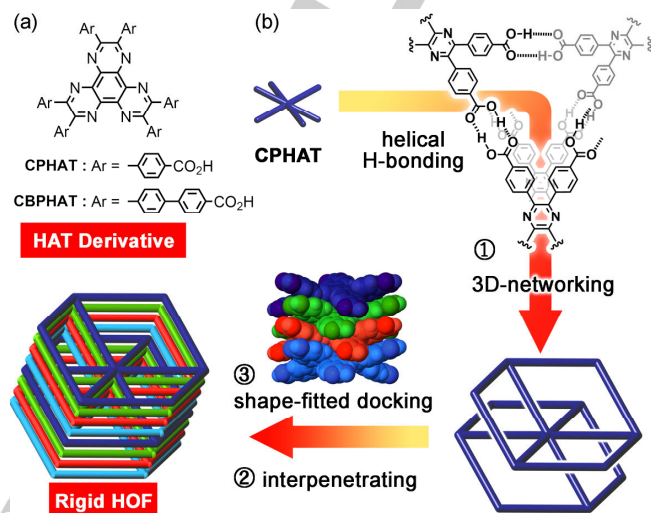


Figure 1. (a) HAT derivatives with carboxyaryl groups (b) Hierarchical interpretation of a stable rigid HOF (CPHAT-1a) through (1) three-dimensional (3D) networking of CPHAT via helical H-bonding, (2) network interpenetration, and (3) shape-fitted docking of twisted HAT cores.

diaminotriazinyl group,^[11] as well as a dimer of carboxy groups which is the most classic and simplest supramolecular synthon.^[12,13]

However, it remains a challenge to obtain sophisticated HOFs with precise crystal structures, large permanent pores, and both chemical and thermal stability. Only a handful of HOFs have been reported with both upper temperature limits of over 200 °C and Brunauer-Emmett-Teller (BET) surface areas [SA_(BET)] of over 1000 m² g⁻¹; these are HOF-TCBP reported by Wu and Yuan et al.,^[12g] trispyrazole derivatives by Miljanic et al.,^[10i,q] IISERP-HOF1 reported by Vaidhyanathan et al.,^[12e] and HOF-5a reported by Chen et al.^[11c] A more generalized strategy is required to achieve such HOFs systematically.

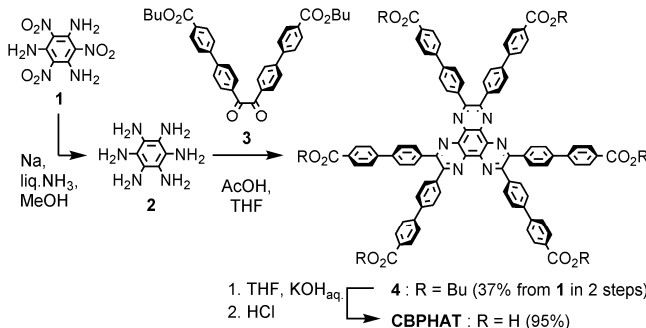
In connection with this, we previously revealed that hexaazatriphenylene (HAT) possessing peripheral carboxyphenyl groups (CPHAT-1) gave a rigid HOF (CPHAT-1a), which achieves a single-crystalline porous structure with significant heat resistance up to 339 °C and SA_(BET) of 649 m² g⁻¹.^[14] As shown in Figure 1, a rigid HOF CPHAT-1a is formed through (1) formation of a three-dimensional (3D) network connected by a H-bonded infinite helical motif, (2) interpenetration of the network, and (3) shape-fitted docking of HAT cores, which seem to be important structural factors to construct highly-stable HOFs with large pores.

Herein, we would like to propose that HAT derivatives possessing peripheral carboxyaryl groups could be a platform to construct highly-stable HOFs with large pores. As a proof of the concept, we demonstrate that an expanded HAT derivative with carboxybiphenyl groups (CBPHAT) gives a stable HOF possessing protic solvent durability, even for conc. HCl, heat resistance up to 305 °C, and a high SA_(BET) of 1288 m² g⁻¹.

[a] Dr. I. Hisaki, Y. Suzuki, Dr. N. Tohnai
Department of Material and Life Science, Graduate School of Engineering, Osaka University, 2-1 Yamadaoka, Suita, Osaka 565-0871 (Japan)
E-mail: hisaki@mls.eng.osaka-u.ac.jp

[b] E. Gomez, Dr. B. Cohen, Prof. Dr. A. Douhal
Departamento de Química Física, Facultad de Ciencias Ambientales y Bioquímica, and INAMOL, Universidad de Castilla-La Mancha, Avenida Carlos III, S/N, 45071 Toledo (Spain)
E-mail: Abderrazzak.Douhal@uclm.es

Supporting information for this article is given via a link at the end of the document.

Scheme 1. Synthesis of **CBPHAT**

Hexaaminobenzene (**2**), which was synthesized by reduction of 1,3,5-triamino-2,4,6-trinitrobenzene (**1**),^[15] was triply condensed with bis(biphenyl)dione derivative **3** under acidic conditions to afford HAT derivative **4** in 37% yield in two steps from **1**. Hydrolysis of **4** gave **CBPHAT** in 95% yield. The synthesized **CBPHAT** was then crystallized by slow evaporation from a solution of *N,N*-dimethylformamide (DMF) and 1,2,4-trichlorobenzene (TCB) at 60 °C to give a pale yellow needle crystalline precipitate denoted as **CBPHAT-1(TCB)**.^[16]

The crystal structure of **CBPHAT-1(TCB)** is shown in Figure 2a, in which **CBPHAT** molecules crystallize into the *P*-3 space group to form a porous hexagonal framework. The carboxy groups form self-complementary H-bonds to give helical strands (Figure 2b). The O1···O3 and O2···O4 distances of the H-bonds are 2.62 and 2.57 Å, respectively. The crystal structure of **CBPHAT-1(TCB)** is isostructural with that of previously reported **CPHAT-1(TCB)** (Figure 2c). **CBPHAT** molecules are one-dimensionally stacked along the *b* axis with a staggered angle of 60° and intermolecular distances of 3.56 Å (Figure 2d). The **CBPHAT** molecule has a twisted conformation due to packing forces; the root mean square deviation (RMSD) of the HAT core is 0.204 Å, which enables shape-fitted docking between adjacent HAT cores. This twisted conformation also makes six peripheral carboxybiphenyl groups alternately directed up and down (torsion angle between the adjacent biphenyl groups is 22.1°), which results in the construction of a 3D H-bonded network with primitive cubic (*pcu*)-topology (Figure 2e). The network is six-fold interpenetrated to give a significantly rigid framework. Three-fold helical channels run along the *b* axis and the channels have a triangular shaped cross section with a width of ca. 14.5 Å; the solvent accessible volume was calculated using the PLATON software^[17] to be 45% (Figure 2f). The channels accommodate TCB molecules, three of which are located in each edge of a triangular channel with disorder into two positions (Figure S1), and the others are located in the center of the channel and are completely disordered.

Thermogravimetric (TG) analysis was conducted to examine the thermal properties (Figure 3a). The TG curve of crystalline bulk of **CBPHAT-1(TCB)** reached a plateau at 180 °C via multi-stepped 53% weight loss and maintained the plateau until the compound began to decompose at around 320 °C. The observed weight loss indicates a host/guest ratio of 1/7, which is also supported by ¹H NMR spectroscopy measurements (Figure

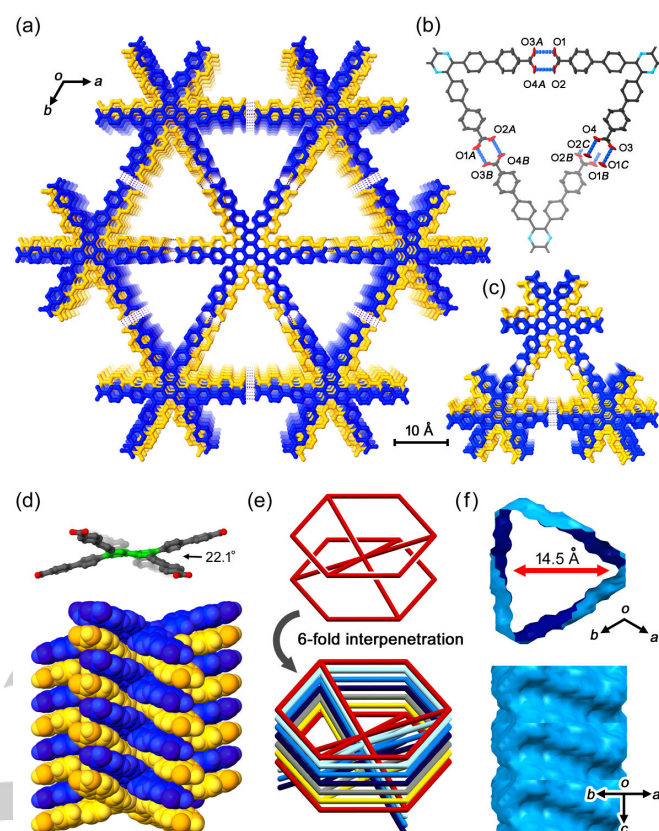


Figure 2. Crystal structure of **CBPHAT-1(TCB)**. Packing diagram of (a) **CBPHAT-1** and (c) **CPHAT-1(TCB)** for reference (CSD Ref Code: MEBKEM). Solvent molecules accommodated in the channel are omitted for clarity. (b) H-bonded three-fold helical strand. Symmetry code: (A) $-x+y, 1-x, 1+z$; (B) $1-y, 1+x-y, 2+z$; (C) $1-y, 1+x-y, -1+z$. (d) (top) Twisted non-planar conformation of **CBPHAT**, where the central HAT moiety is colored green, and (bottom) its shape-fitted 1D-stacked column. (e) Schematic models of (top) single and (bottom) six-fold interpenetrated frameworks with *pcu* topology. (f) Visualization of the helical channel surface.

S2). To obtain structural information during desolvation by heating, variable temperature-powder X-ray diffraction (VT-PXRD) patterns of bulk crystalline **CBPHAT-1(TCB)** were recorded while heating from room temperature to 360 °C (Figure 3b). The diffraction intensity of the 100 peak was also plotted (Figure 3c). As observed in other previously reported systems,^[13c,14] the peak intensity was poor in the low temperature region (r.t. to 100 °C) because of disordered TCB molecules inside the channels. Disordered TCB molecules were removed by heating, so that the peak intensity increased and reached a plateau at 126 °C. It is noteworthy that the observed PXRD pattern, which is in good agreement with that of **CBPHAT-1(TCB)**, was retained up to 305 °C, which indicates that the framework shows no structural changes upon desolvation, and that it has significantly high temperature resistance.

Activation of **CBPHAT-1(TCB)** was accomplished at 150 °C under vacuum condition for 24 h to yield the activated crystalline

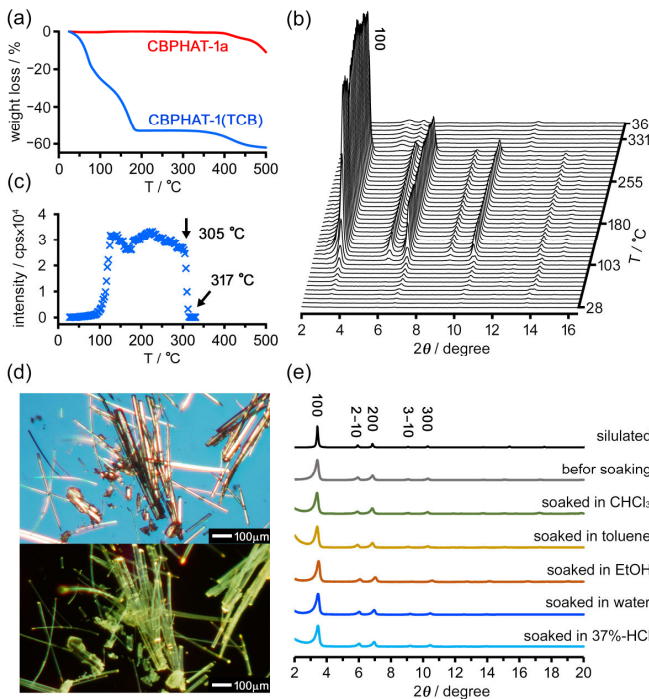


Figure 3. Thermal and chemical durability of crystalline **CBPHAT-1a**. (a) TG profiles of **CBPHAT-1(TCB)** (blue line) and **CBPHAT-1a** (red line). (b) VT-PXRD patterns of **CBPHAT-1(TCB)** heated from r.t. to 360 °C. (c) Changes of the 100 peak intensity with temperature. The intensity rapidly decreased at 305–317 °C, which indicated collapse of the framework. (d) POM micrographs of **CBPHAT-1a** under ambient light (top) and UV light with a wavelength of 365 nm. (e) PXRD patterns of **CBPHAT-1a** simulated from SXRD data, before soaking, and after soaking in hot solvents for 7 days: CHCl_3 (60 °C), toluene (100 °C), ethanol (60 °C), water (100 °C), and 37% HCl (60 °C).

material **CBPHAT-1a**. Complete desolvation was confirmed by TG analysis (Figure 3a) and ^1H NMR spectroscopy (Figure S3). **CBPHAT-1a** retained single crystallinity, as indicated by polarized optical microscopy (POM) observation (Figure 3d), and SXRD analysis of **CBPHAT-1a** was successfully accomplished. **CBPHAT-1a** has the same framework as **CBPHAT-1(TCB)** (Table S1), although a very slight increase of the a , b and c axes was observed. The framework of **CBPHAT-1a** resisted protic solvents, which would typically cleave the H-bonds.^[18] PXRD patterns of **CBPHAT-1a** shown in Figure 3e retain the original profile after soaking in chloroform at 60 °C, toluene at 100 °C, ethanol at 60 °C, water at 100 °C, and 37% HCl at 60 °C for 7 days. However, alkaline aqueous solution, such as KOH, immediately dissolved the crystalline powder of **CBPHAT-1a**, which is the durability limitation of HOFs connected by the dimerization of carboxy groups.

The permanent porosity of **CBPHAT-1a** was evaluated from N_2 , O_2 , CO_2 , and H_2 gas sorption experiments at 77, 195, 77, and 77 K, respectively (Figure 4a). **CBPHAT-1a** has a type-I N_2 sorption isotherm with an uptake of $362 \text{ cm}^3 \text{ g}^{-1}$ at 101 kPa. The $\text{SA}_{(\text{BET})}$ and pore size calculated using non-local density functional theory (NLDFT) for the N_2 isotherm were $1288 \text{ m}^2 \text{ g}^{-1}$ and 1.2 nm, respectively (Figures 4b and 4S). Uptakes of other gases were $427 \text{ cm}^3 \text{ g}^{-1}$ for O_2 at 20 kPa, $305 \text{ cm}^3 \text{ g}^{-1}$ for CO_2 at 100 kPa, and $111 \text{ cm}^3 \text{ g}^{-1}$ (1 wt%) for H_2 at 102 kPa. Compared

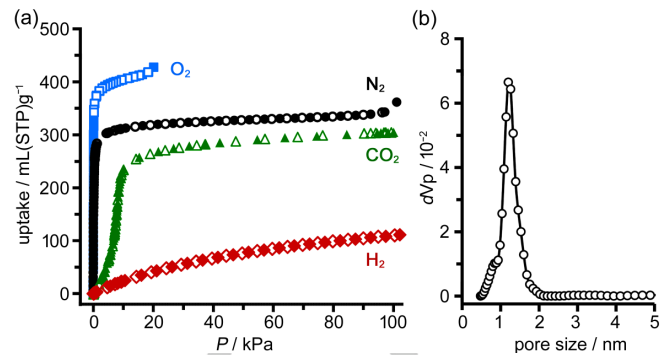


Figure 4. (a) Gas sorption isotherms of **CBPHAT-1a**: O_2 (77 K), N_2 (77 K), CO_2 (195 K), H_2 (77 K). Filled symbols: absorption process, open symbols: desorption process. (b) Pore size distribution calculated by the NLDFT method.

Table 1. Comparison of **CPHAT-1a** and **CBPHAT-1a**

	CPHAT-1a	CBPHAT-1a
Network topology	pcu	pcu
Number of interpenetrated networks	4	6
Pore size / Å	6.4	14.5
Void ratio ^[a]	31%	45%
Upper temperature limit / °C	339	305
$\text{SA}_{(\text{BET})} / \text{m}^2 \text{ g}^{-1}$	649 ^[a]	1288

[a] The value was estimated by PLATON software^[17].

with O_2 and N_2 , the isotherm for CO_2 increased relatively gently in the low pressure region (<7 kPa).

A comparison of the structural parameters of **CBPHAT-1a** and the previously reported **CPHAT-1a** is given in Table 1. As expected, **CBPHAT-1a** has a similar molecular conformation, hydrogen-bonded framework, 1D stacking columns, and hexagonal arrangements of the columns, while the number of intercalated frameworks is different due to the length of the arms (four-fold for **CPHAT-1a** and six-fold for **CBPHAT-1a**). By expansion of the aryl arm, the width of pore, the void ratio and $\text{SA}_{(\text{BET})}$ are increased from 6.4 Å, 31%, and $649 \text{ m}^2 \text{ g}^{-1}$ to 14.5 Å, 45%, and $1288 \text{ m}^2 \text{ g}^{-1}$, respectively. The formation of isostructural porous frameworks is quite rare for HOF systems,^[19] which indicates that the present HAT system can be used as a platform to construct isostructural HOFs with different void sizes.

The bulk of **CBPHAT-1a** and its butyl ester derivative (4) show a broad absorption band between 300 and 500 nm, and a green-yellow emission with intensity maxima around 500 nm (Figures S5 and S6). The fluorescence quantum yield of the HOF is 5.7%. Fluorescence confocal microscopy measurements on **CBPHAT-1a** single crystals showed highly anisotropic emission behavior (Figures 5a and b). The anisotropy histogram for the crystals oriented perpendicularly to the plane of observation has a value of 0.45, while those rotated by 90° (parallel orientation) give a value of -0.30. Similar anisotropy

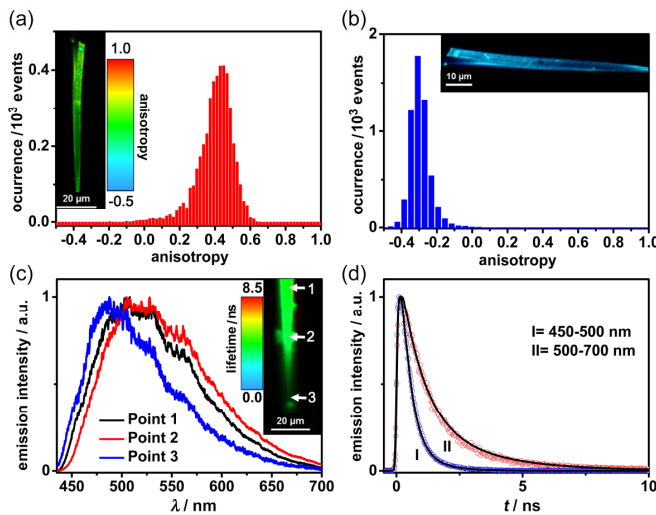


Figure 5. Fluorescence properties of **CBPHAT-1a** single crystals. a) and b) Histograms of the emission anisotropy for 2 positions of **CBPHAT-1a** crystal. The insets show images of the crystals. c) Emission spectra at different points of a **CBPHAT-1a** crystal. The inset shows an image of the crystal and the points of measurement. d) Fluorescence decay of a **CBPHAT-1a** crystal; the I and II decays were measured using FF01-470_28-25 and HQ550LP filters (Chroma).

behavior has been reported for **CPHAT-1a**.^[14] This strong dependence of the anisotropy on the crystal orientation indicates an ordered crystalline structure for **CBPHAT-1a** with preferential orientation of the molecular dipole moments perpendicular to the long crystal axis with the π - π columnar stacking direction parallel to the length axis of the crystal. The emission spectra of **CBPHAT-1a** do much not vary between the different crystals, although they do change depending on the position within each crystal. At the center, the spectra have emission intensity maxima at ca. 475 nm (Figure 5c), while those collected close to the edges shift to redder wavelengths (ca. 510 nm) and become broader. This behavior is explained in terms of the presence of structural defects along the edges of the crystals. The emission decays of **CBPHAT-1a** single crystals collected in the blue (450–500 nm) and green/red (550–660 nm) region of the spectrum give lifetimes of $\tau_1 \sim 0.4$ ns (94%) and $\tau_2 \sim 1.2$ ns (6%), and $\tau_1 \sim 1.1$ ns (80%) and $\tau_2 \sim 2.7$ ns (20%), respectively (Figure 5d). The lifetimes in the blue and green/red emission ranges are comparable to those reported for **CPHAT-1a**, which suggests that the emitters from both crystals in this spectral region are very similar in nature.^[14] The only notable difference is the decrease in the value of the longest component from 4.5 ns for **CPHAT-1a** to 2.7 ns for **CBPHAT-1a**. This component is associated with the interactions between the building units of the crystals and the decrease can be explained in terms of the stronger interactions due to the presence of the additional carboxyphenyl groups in **CBPHAT-1a**. Thus, the expansion of the aryl arm in **CBPHAT-1a** and the change in the pore size did not significantly alter the optical and photophysical properties of the resultant HOF structure.

In conclusion, we demonstrated that a HAT-based docking methodology can be a useful strategy to construct significantly thermostable crystalline HOFs with large surface areas. The

derivative with carboxybiphenyl groups (**CBPHAT**) yields a significantly stable single-crystalline porous HOF (**CBPHAT-1a**) with protic solvent durability, even for conc. HCl, heat resistance up to 305 °C, and a high $SA_{(BET)}$ of 1288 m² g⁻¹. To explore HOFs with larger pores and more stability, HAT derivatives with various longer aryl groups are under investigation in our laboratory.

Acknowledgements

This work was supported by Grant-in-Aid for Scientific Research Projects from Japan (KAKENHI; JPT15K04591 and JPTA18H019660), and from Spain (MINECO; MAT2014-57646-P). Preliminarily crystal structure analysis was conducted using the BL38B1 at SPring-8 with approval of the Japan Synchrotron Radiation Research Institute (JASRI) (Proposal Nos. 2017A1211 and 2017B1322). E.G. thanks the MINECO for the PhD fellowship: FPU15/01362.

Keywords: porous organic framework • hydrogen bond • carboxylic acid • fluorescence • crystal engineering

References and Notes

- [1] A. G. Slater, A. I. Cooper, *Science*, **2015**, 348, aaa8075.
- [2] a) A. Comotti, A. Bracco, P. Sozzani, *Acc. Chem. Res.* **2016**, 49, 1701–1710; b) S. Das, P. Heasman, T. Ben, S. Qiu, *Chem. Rev.* **2017**, 117, 1515–1563.
- [3] a) A. P. Côté, A. I. Benin, N. W. Ockwig, M. O’Keeffe, A. J. Matzger, O. M. Yaghi, *Science*, **2005**, 310, 1166–1170; b) P. J. Waller, F. Gándara, O. M. Yaghi, *Acc. Chem. Res.* **2015**, 48, 3053–3063.
- [4] a) X. Feng, X. Ding, D. Jiang, *Chem. Soc. Rev.* **2012**, 41, 6010–6022; b) S.-Y. Ding, W. Wang, *Chem. Soc. Rev.* **2013**, 42, 548–568; c) M. Dogru, T. Bein, *Chem. Commun.* **2014**, 50, 5531–5546; d) W. Zhao, L. Xia, X. Liu, *CrystEngComm* **2018**, 20, 1613–1634.
- [5] V. Nguyen, M. Grünwald, *J. Am. Chem. Soc.* **2018**, 140, 3306–3311.
- [6] Some excellent COF systems with high crystallinity are reported. See, for example: a) D. Beaudoin, T. Maris, J. D. Wuest, *Nat. Chem.* **2013**, 5, 830–834; b) P. Kissel, D. J. Murray, W. J. Wulf lange, V. J. Catalano, B. T. King, *Nat. Chem.* **2014**, 6, 774–778; c) M. J. Kory, M. Wörle, T. Weber, P. Payamyr, S. W. van de Poll, J. Dshemuchadse, N. Trapp, A. D. Schlüter, *Nat. Chem.* **2014**, 6, 779–784; d) L. Ascherl, T. Sick, J. T. Margraf, S. H. Lapidus, M. Calik, C. Hettstedt, K. Karaghiosoff, M. Döblinger, T. Clark, K. W. Chapman, F. Auras, T. Bein, *Nat. Chem.* **2016**, 8, 310–316.
- [7] For precise structural study based on theoretical calculation, see. B. Lukose, A. Kuc, T. Heine, *Chem. Eur. J.* **2011**, 17, 2388–2392.
- [8] Review for HOFs, see; J. Lu, R. Cao, *Angew. Chem. Int. Ed.* **2016**, 55, 9474–9480; *Angew. Chem.* **2016**, 128, 9624–9630.
- [9] For supramolecular synthon, see: G. R. Desiraju, *Angew. Chem., Int. Ed. Engl.* **1995**, 34, 2311–2327; *Angew. Chem.* **1995**, 107, 2541–2558.
- [10] a) A. R. A. Palmans, J. A. J. M. Vekemans, H. Kooijman, A. L. Spek, E. W. Meijer, *Chem. Commun.* **1997**, 2247–2248; b) P. Sozzani, A. Comotti, R. Simonutti, T. Meersmann, J. W. Logan, A. Pines, *Angew. Chem. Int. Ed.* **2000**, 39, 2695–2698; *Angew. Chem.* **2000**, 112, 2807–2810; c) B. K. Saha, R. K. R. Jetti, K. S. Reddy, S. Aitipamula, A. Nangia, *Cryst. Growth Des.* **2005**, 5, 887–899; d) K. E. Maly, E. Gagnon, T. Maris, J. D. Wuest, *J. Am. Chem. Soc.* **2007**, 129, 4306–4322; e) J. Yang, M. B. Dewal, S. Profeta, Jr., M. D. Smith, Y. Li, L. S. Shimizu, *J. Am. Chem. Soc.* **2008**, 130, 612–621; f) A. Comotti, S. Bracco, G. Distefano, P. Sozzani, *Chem. Commun.* **2009**, 284–286; g)

W. Yang, A. Greenaway, X. Lin, R. Matsuda, A. J. Blake, C. Wilson, W. Lewis, P. Hubberstey, S. Kitagawa, N. R. Champness, M. Schröder, *J. Am. Chem. Soc.* **2010**, *132*, 14457–14469; h) M. Mastalerz, I. Oppel, *Angew. Chem. Int. Ed.* **2012**, *51*, 5252–5255; *Angew. Chem.* **2000**, *124*, 5345–5348; i) X.-Z. Luo, X.-J. Jia, J.-H. Deng, J.-L. Zhong, H.-J. Liu, K.-J. Wang, D.-C. Zhong, *J. Am. Chem. Soc.* **2013**, *135*, 11684–11687; j) T.-H. Chen, I. Popov, W. Kaveevivitchai, Y.-C. Chuang, Y.-S. Chen, O. Daugulis, A. J. Jacobson and O. Š. Miljanic, *Nat. Commun.*, **2014**, *5*, 5131; k) J. Lü, C. Perez-Krap, M. Suyetin, N. H. Alsmail, Y. Yan, S. Yang, W. Lewis, E. Bichoutskaia, C. C. Tang, A. J. Blake, R. Cao, M. Schröder, *J. Am. Chem. Soc.* **2014**, *136*, 12828–12831; l) A. Comotti, S. Bracco, A. Yamamoto, M. Beretta, T. Hirukawa, N. Tohnai, M. Miyata, P. Sozzani, *J. Am. Chem. Soc.* **2014**, *136*, 618–621; m) P. Li, Y. He, Y. Zhao, L. Weng, H. Wang, R. Krishna, H. Wu, W. Zhou, M. O'Keeffe, Y. Han and B. Chen, *Angew. Chem. Int. Ed.* **2015**, *54*, 574–577; *Angew. Chem.* **2015**, *127*, 584–587; n) V. N. Yadav, A. Comotti, P. Sozzani, S. Bracco, T. Bonge-Hansen, M. Hennum, C. H. Görbitz, *Angew. Chem. Int. Ed.* **2015**, *54*, 15684–15688; *Angew. Chem.* **2015**, *127*, 15910–15914; o) Y. Zhou, B. Liu, X. Sun, J. Li, G. Li, Q. Huo, Y. Liu, *Cryst. Growth Des.* **2017**, *17*, 6653–6659; p) S. Bracco, T. Miyano, M. Negroni, I. Bassanetti, L. Marchio', P. Sozzani, N. Tohnai, A. Comotti, *Chem. Commun.* **2017**, *53*, 7776–7779; q) M. I. Hashim, H. T. M. Le, T.-H. Chen, Y.-S. Chen, O. Daugulis, C.-W. Hsu, A. J. Jacobson, W. Kaveevivitchai, X. Liang, T. Makarenko, O. Š. Miljanic, I. Popovs, H. V. Tran, X. Wang, C.-H. Wu, J. I. Wu, *J. Am. Chem. Soc.* **2018**, *140*, 6014–6026.

[11] a) Y. He, S. Xiang, B. Chen, *J. Am. Chem. Soc.* **2011**, *133*, 14570–14573; b) H. Wang, B. Li, H. Wu, T.-L. Hu, Z. Yao, W. Zhou, S. Xiang, B. Chen, *J. Am. Chem. Soc.* **2015**, *137*, 9963–9970; c) W. Yang, B. Li, H. Wang, O. Alduhaish, K. Alfooty, M. A. Zayed, P. Li, H. D. Arman, B. Chen, *Cryst. Growth Des.* **2015**, *15*, 2000–2004.

[12] a) D. J. Duchamp, R. Marsh, *Acta Crystallogr. B* **1969**, *25*, 5–19; b) F. H. Herbstein, M. Kapon, G. M. Reisner, *J. Inclusion Phenom.* **1987**, *5*, 211–214. (c) K. Kobayashi, T. Shirasaka, E. Horn, N. Furukawa, *Tetrahedron Lett.* **2000**, *41*, 89–93; d) C. A. Zentner, H. W. H. Lai, J. T. Greenfield, R. A. Wiscons, M. Zeller, C. F. Campana, O. Talu, S. A. Fitzgerald, J. L. C. Rowsell, *Chem. Commun.* **2015**, *51*, 11642–11645; e) S. Nandi, D. Chakraborty, R. Vaidyanathan, *Chem. Commun.* **2016**, *52*, 7249–7252; f) I. Hisaki, N. Q. E. Affendy, N. Tohnai, *CrystEngComm* **2017**, *19*, 4892–4898; g) F. Hu, C. Liu, M. Wu, J. Pang, F. Jiang, D. Yuan, M. Hong, *Angew. Chem.* **2017**, *129*, 2133–2136; *Angew. Chem. Int. Ed.* **2017**, *56*, 2101–2104; h) W. Yang, J. Wang, H. Wang, Z. Bao, J. C.-G. Zhao, B. Chen, *Cryst. Growth Des.* **2017**, *17*, 6132–6137.

[13] a) I. Hisaki, S. Nakagawa, N. Tohnai, M. Miyata, *Angew. Chem. Int. Ed.* **2015**, *54*, 3008–3012; *Angew. Chem.* **2015**, *127*, 3051–3055; b) I. Hisaki, N. Ikenaka, N. Tohnai, M. Miyata, *Chem. Commun.* **2016**, *52*, 300–303; c) I. Hisaki, S. Nakagawa, N. Ikenaka, Y. Imamura, M. Katouda, M. Tashiro, H. Tsuchida, T. Ogoshi, H. Sato, N. Tohnai, M. Miyata, *J. Am. Chem. Soc.* **2016**, *138*, 6617–6628; d) I. Hisaki, S. Nakagawa, H. Sato, N. Tohnai, *Chem. Commun.* **2016**, *52*, 9781–9784; e) I. Hisaki, H. Toda, H. Sato, N. Tohnai, H. Sakurai, *Angew. Chem. Int. Ed.* **2017**, *56*, 15294–15298; *Angew. Chem.* **2017**, *129*, 15496–15500.

[14] I. Hisaki, N. Ikenaka, E. Gomez, B. Cohen, N. Tohnai, A. Douhal, *Chem. Eur. J.* **2017**, *23*, 11611–11619.

[15] D. Z. Rogers, *J. Org. Chem.* **1986**, *51*, 3904–3905.

[16] Crystal data for **CBPHAT-1(TCB)**: $(C_{90}H_{54}N_6O_{12}) \cdot 3(C_6H_3Cl_3)$, $F_w = 1955.70$, $a = b = 29.7532(15)$ Å, $c = 7.1146(6)$ Å, $\alpha = \beta = 90^\circ$, $\gamma = 120^\circ$, $V = 5454.4(6)$ Å³, $T = 93$ K, trigonal, space group *P*-3, $Z = 2$, 29812 collected, 7251 unique ($R_{int} = 0.097$) reflections, the final $R1$ and $wR2$ values 0.130 ($I > 2.0\sigma(I)$) and 0.385 (all data), respectively. Crystal data for **CBPHAT-1a**: $C_{90}H_{54}N_6O_{12}$, $F_w = 1411.45$, $a = b = 29.7810(10)$ Å, $c = 7.1709(3)$ Å, $\alpha = \beta = 90^\circ$, $\gamma = 120^\circ$, $V = 5507.9(3)$ Å³, $T = 93$ K, trigonal, space group *P*-3, $Z = 2$, 16474 collected, 7205 unique ($R_{int} = 0.075$) reflections, the final $R1$ and $wR2$ values 0.078 ($I > 2.0\sigma(I)$) and 0.241 (all data). CCDC1841012 [**CBPHAT-1(TCB)**] and CCDC1841011 (**CBPHAT-1a**) contain the supplementary crystallographic data for this paper. These data are provided free of charge by The Cambridge Crystallographic Data Centre.

[17] A. L. Spek, *Acta Crystallogr. Sect. D* **2009**, *65*, 148–155.

[18] **CBPHAT-1a** is figurally soluble in dichloromethane and moderately soluble in DMF.

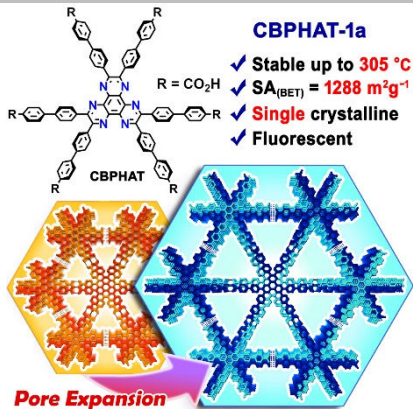
[19] Recently isostructural HOFs with large pores is reported, see ref. 10q.

Entry for the Table of Contents (Please choose one layout)

Layout 1:

COMMUNICATION

We demonstrated that HAT derivatives are a suitable building block for the systematic construction of stable hydrogen-bonded framework, and that the derivative with carboxybiphenyl groups forms a stable single-crystalline porous framework (**CBPHAT-1a**) that possesses protic solvent durability, heat resistance up to 305 °C, and $SA_{(BET)}$ of 1288 $m^2 g^{-1}$.



I. Hisaki,* Y. Suzuki, E. Gomez, B. Cohen, N. Tohnai, A. Douhal*

Page No. – Page No.

Docking Strategy to Construct Thermostable, Single-crystalline, Hydrogen-bonded Organic Framework with Large Surface Area